

Processing seismic data for high spatial resolution

John C. Bancroft, Helen Isaac, and Nassir Saeed

ABSTRACT

High spatial resolution has been observed on the Hussar data that shows apparent faulting. We propose that this high resolution results from processing the data with common scatterpoint gathers that allow high resolution velocity analysis, combined with velocity modifications that allow the focusing of reflections that come from reflectors that are oblique to the 2D line. To date, we have not been able to replicate this spatial resolution with conventional methods.

INTRODUCTION

High spatial resolution of data from the Hussar project was created using common scatter point (CSP) gathers using equivalent offset migration. The resolution of this data appears to be unmatched by other processing schemes. Our investigations lead us to believe that it is the unique velocity analysis of the CSP gathers that allows this high resolution. These velocities are able to match the apparent change of the medium velocity when static shifts are applied to the data.

Reflectors that are oblique to a 2D line produce reflections that require a special velocity that compensates for the angle of obliquity.

Velocity analysis of CSP gathers tend to be more structured than expected for the relatively flat area of Hussar, Alberta. We propose that it is the unique capability of forming the CSP gathers that allow the picked velocities to contain corrections induced by static variations.

THEORY

Prestack migrations are more sensitive to velocities than poststack migrations. This sensitivity can be used to aid in estimating the subsurface structure. These velocities are modified when moving data to the processing datum. “Rules of thumb” have indicated that elevation changes from surface to datum can be accomplished using vertical static corrections when the elevation changes are less than 3 to 5 trace intervals. For conventional data, this assumes that elevations which vary from 100 to 150 m can be processed with vertical static corrections to the datum. This rule of thumb assumed that this slight time variation had little effect on the velocity used for moveout correction and migration.

Common scatterpoint gathers are formed by moving all input traces, within the migration aperture, to an offset that preserves the travel time from a scatterpoint. These offsets are based on the raypath geometry, and not solely on the source-receiver offset.

Velocity sensitivity to statics

A velocity sensitivity test was created to evaluate the apparent change in the velocity required for focusing the data when a static time shift was applied. The test assumed an

RMS velocity $V_{RMS} = 3000.0$ m/s and test points located at zero-offset times $T_0 = 0.4 : 0.1 : 1.5$ sec. The time T to an offset h was computed using the hyperbolic moveout equation.

$$T^2 = T_0^2 + \frac{4h^2}{V_{RMS}^2} . \quad (1)$$

An array of small elevation changes from -100 to 100 meters was created to simulate elevation changes, and from these elevation changes a two-way time static δt was computed, i.e.,

$$\delta t = \frac{2 * \delta z}{V_{RMS}} . \quad (2)$$

This static was applied to each T as illustrated in Fig. 1. The shifted hyperbola does not fit the form of equation (1), so a correct form with a new velocity V_{New} is defined by using a point at offset h .

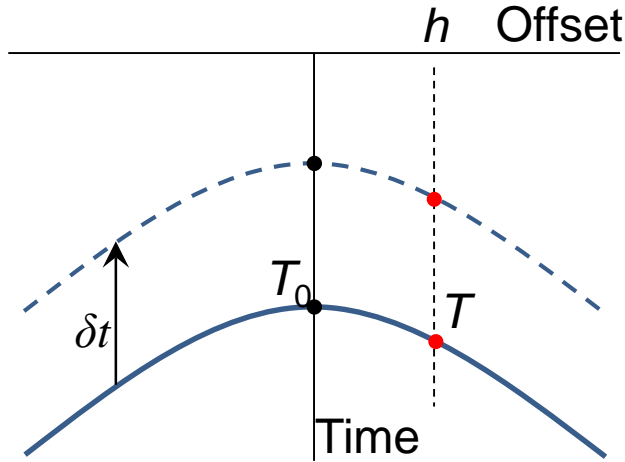


Fig. 1: Illustration of hyperbola and the shifted hyperbola.

The apparent new velocity V_{New} was computed using

$$V_{New} \approx V_{RMS} \sqrt{\frac{T_0}{T_0 - \delta t}}, \quad (3)$$

where δt is the time shift for the static correction. (See companion paper in this report with title “The sensitivity of velocities with elevation change.”)

The new velocity V_{New} versus time shift is displayed in Fig. 2. for various T_0 's.

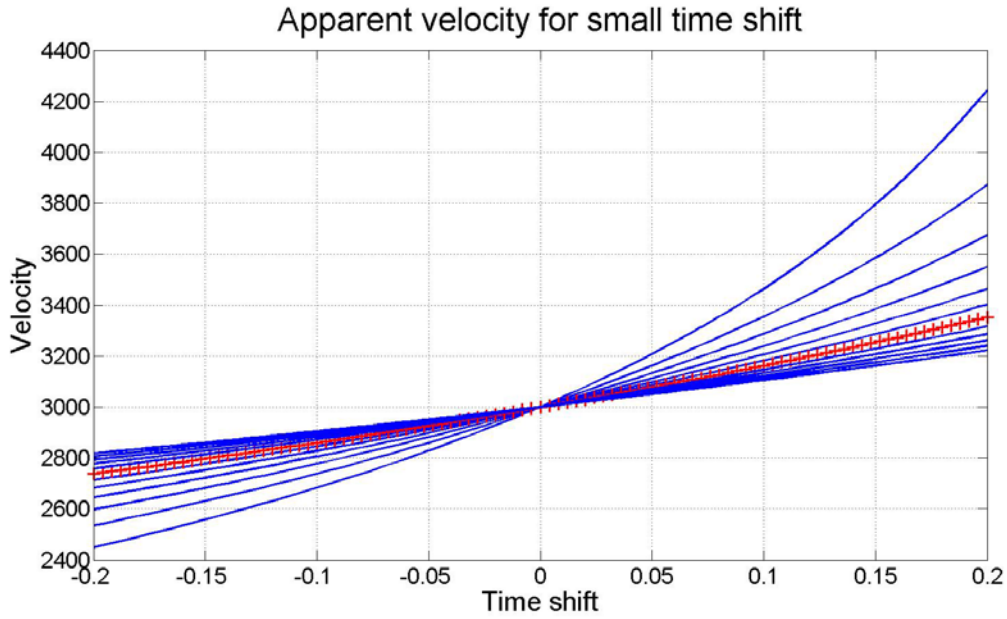


Fig. 2: Apparent velocity (m/s) versus change time shift (s) due to static corrections. Each curve represents various T_0 's that range from 0.4 to 1.5 sec. The red "+" signs are for $T_0 = 1.0$ sec.

For static changes of 0.050 s, at $T_0 = 1.0$ sec, the new velocity is approximately 3080 m/s.

Oblique reflectors

Oblique reflectors may be imaged using velocities V_{Obl} that is defined from

$$V_{Obl} = \frac{V_{RMS}}{\cos(\gamma)}, \quad (4)$$

where γ is the oblique angle of the reflector measured from the normal to the seismic line. Migrating the data with increasing velocities allows oblique reflections to be focused. Knowing the velocity that best focuses the reflection allow the oblique angle to be estimated.

HUSSAR DATA

Velocity analysis of CSP gathers

A P-P data set from the Hussar project was chosen and preprocessed to a median elevation. CSP gathers were created using a single velocity function. These gathers are formed without time shifting to preserve moveout defined with RMS velocities. Moveout correction, scaling, and muting complete the prestack migration.

The elevation of the Hussar 2D seismic line is displayed in Fig. 3.

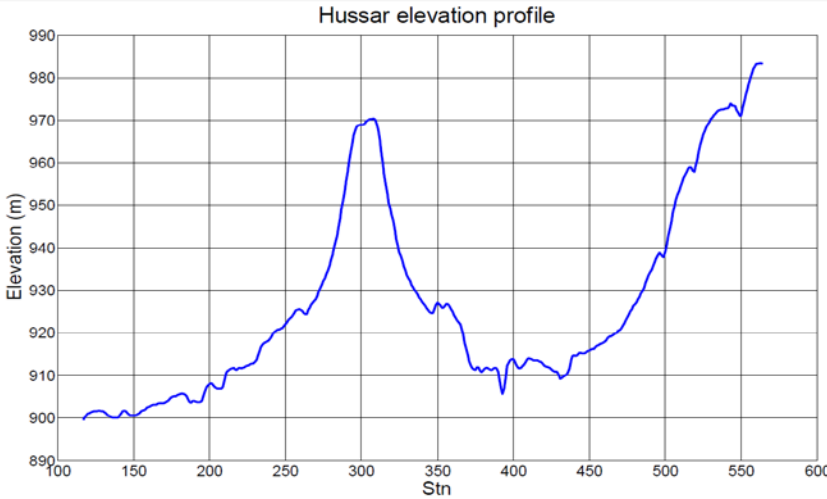


Fig. 3: Elevation profile of the Hussar line.

The velocity field for the Hussar data which was used in producing the high resolution data is displayed in Fig. 4. These velocities were picked on every 50th CSP gather.

We believe that it is these accurate velocities that produce the spatial high resolution data. These velocities do-not represent the actual subsurface velocities which we assume would be relatively horizontal. We assume that these velocities compensate for time shifts that are required to remove the effect of surface elevation and near surface anomalies when moving the data to a horizontal datum.

The red line in Fig. 4 identifies two different velocities at 600 ms. These velocities are considerable different and are approximately 2100 and 2800 m/s.

Oblique reflectors

A CREWES paper (Bancroft, et al., 2011) described the imaging of reflectors that are at an oblique angle to a 2D seismic line. In essence, the prestack migration velocity is increased to a value that “best” focuses the oblique reflection.

Increasing these velocities by a constant scale factor appears to improve the focusing of oblique reflectors. The first image in Figure 5 shows the data processed to 4 seconds with the estimated velocity field. Some faults do appear on this section, and, as expected are imaged slightly below the median time of 2.0 sec.

The CSP gathers are then processed with velocities V_{Obl} that increase in increments from 100, 110, 120, 125, 130, 140, 160, 180, and 200 percent of the picked velocities. These results are shown in Fig. 6 to Fig. 14, which only display the first two seconds of data. Faults appear to focus at different percentage of velocities, indicating their angle of obliquity γ may vary.

Slight faulting may be observed in Fig. 5 around 2.0 sec. and between CDP’s 536 and 636. This area of faulting becomes more defined in Fig. 12 where the velocity is $1.6V_{Rms}$. If this is the best focusing, then the angle of obliquity is approximately 50 degrees. Other faults or discontinuities may focus at different velocities.

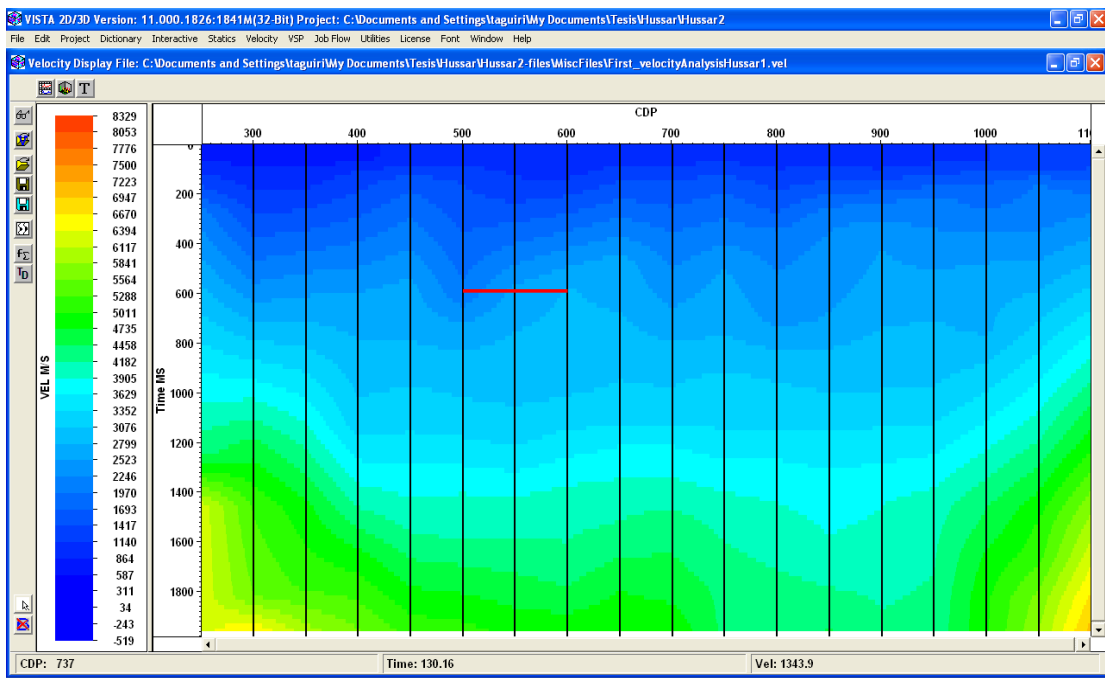


Fig. 4: Velocity field used in producing the high spatial resolution data.

Prestack migration images

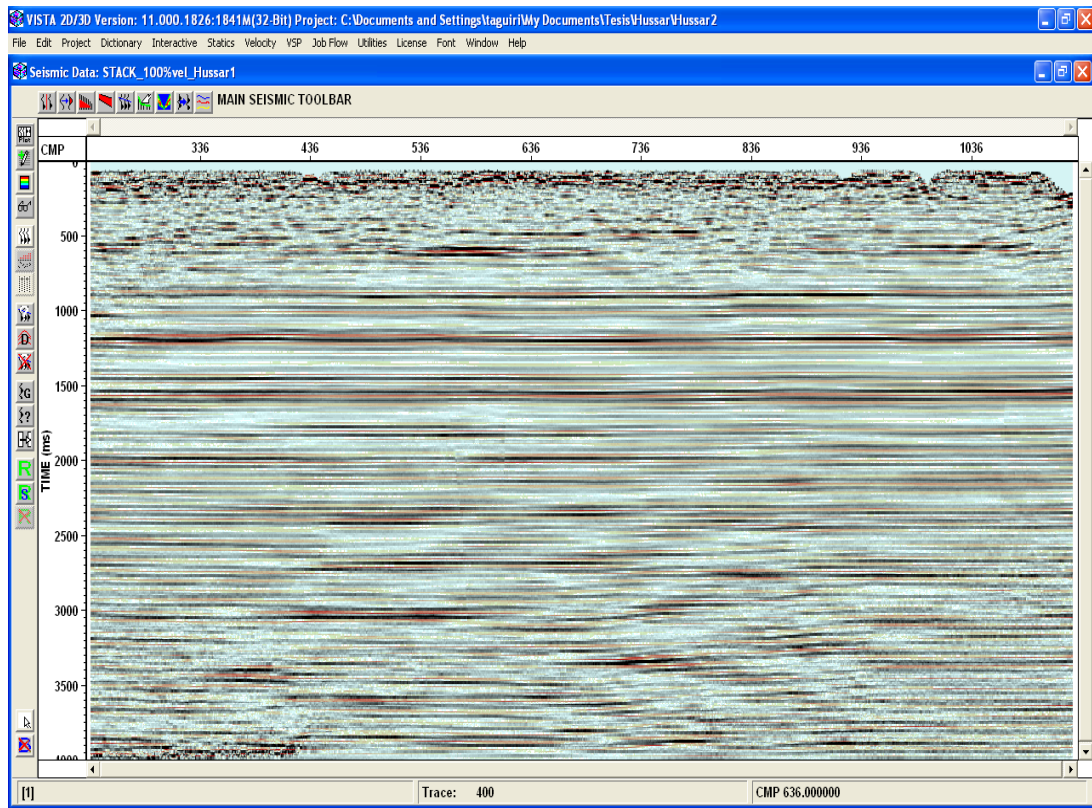


Fig. 5: Hussar data processed to 4.0 sec. using **100%** of the picked velocities.

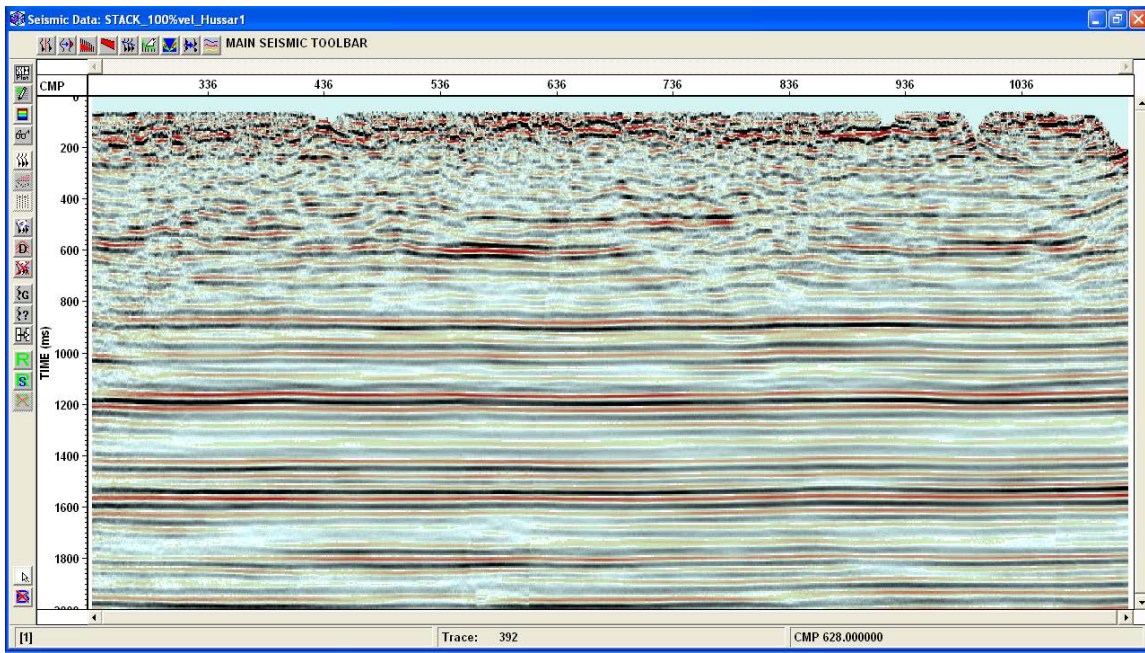


Fig. 6: Hussar data processed to 2.0 sec. using **100%** of the picked velocities.

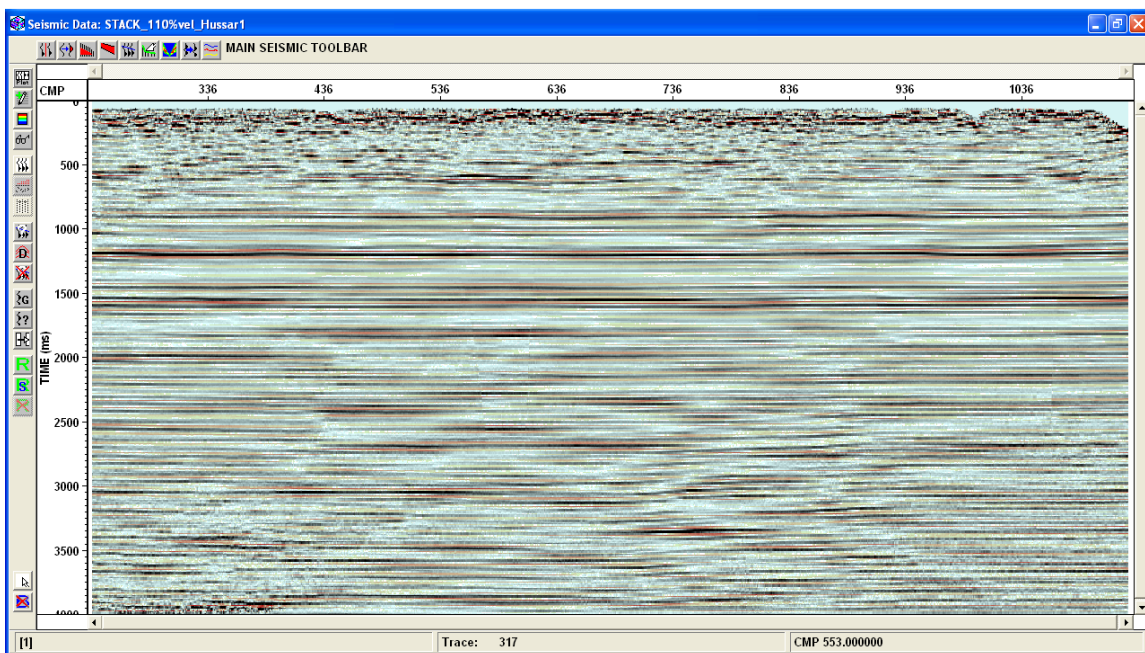


Fig. 7: Hussar data processed to 2.0 sec. using **110%** of the picked velocities.

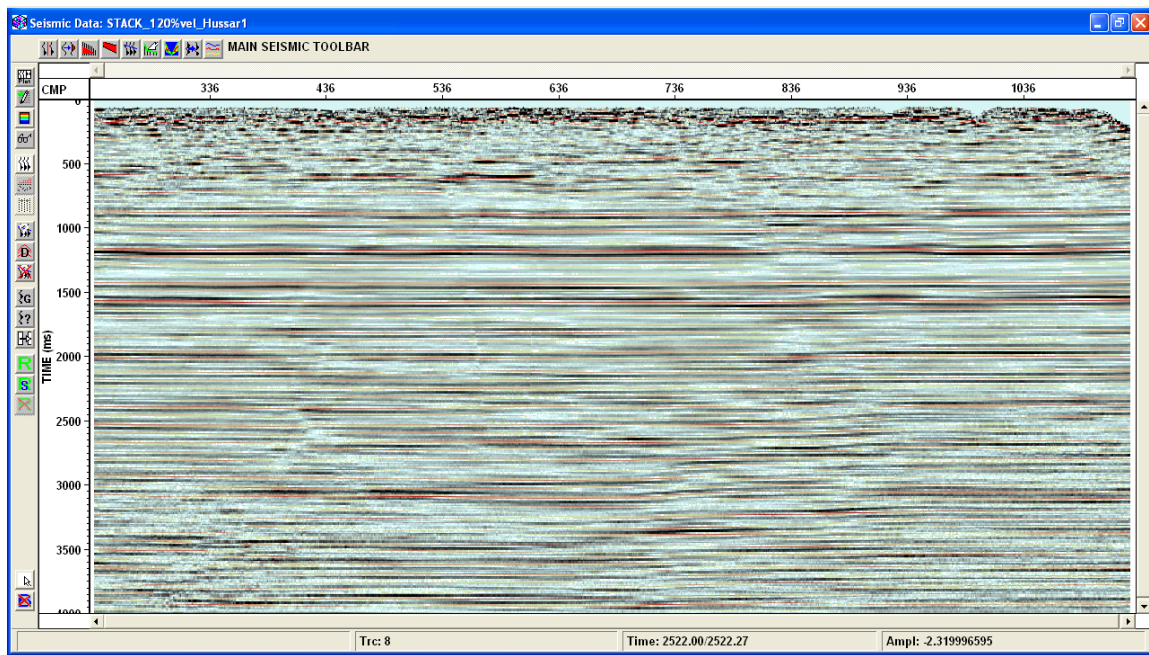


Fig. 8: Hussar data processed to 2.0 sec. using **120%** of the picked velocities.

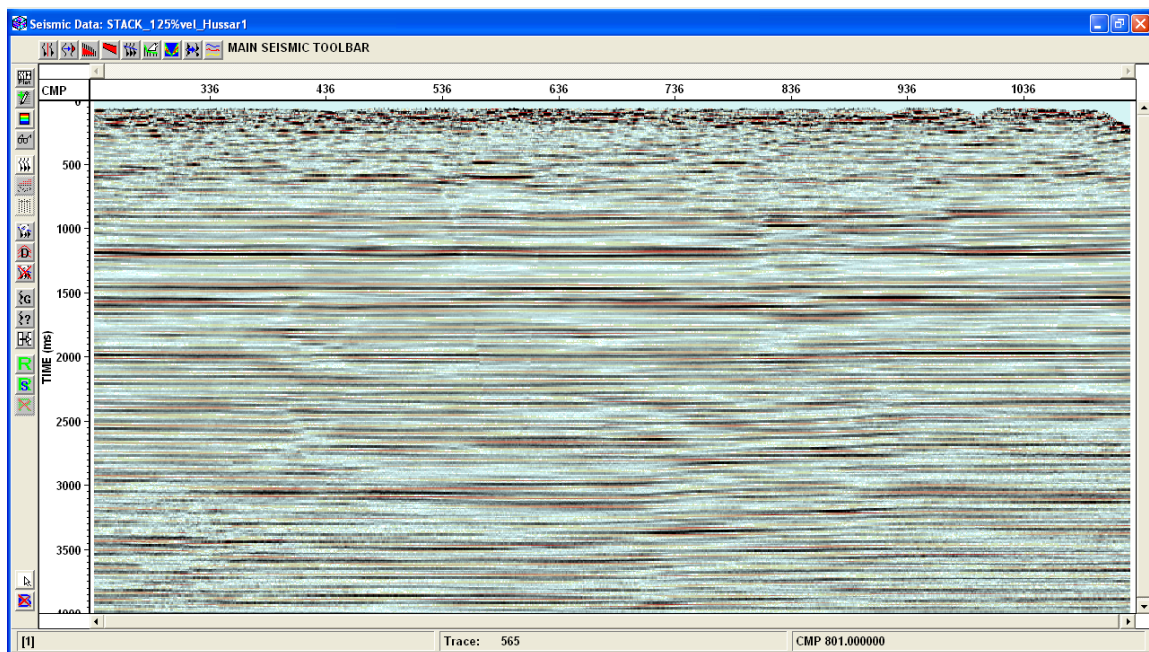


Fig. 9: Hussar data processed to 2.0 sec. using **125%** of the picked velocities.

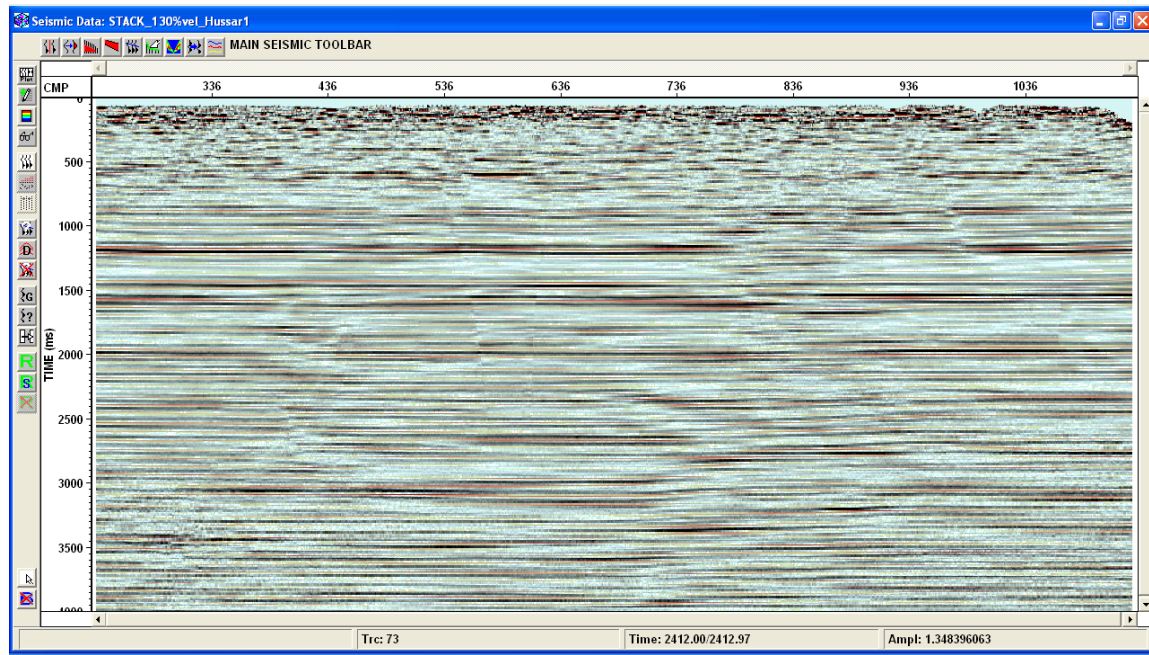


Fig. 10: Hussar data processed to 2.0 sec. using **130%** of the picked velocities.

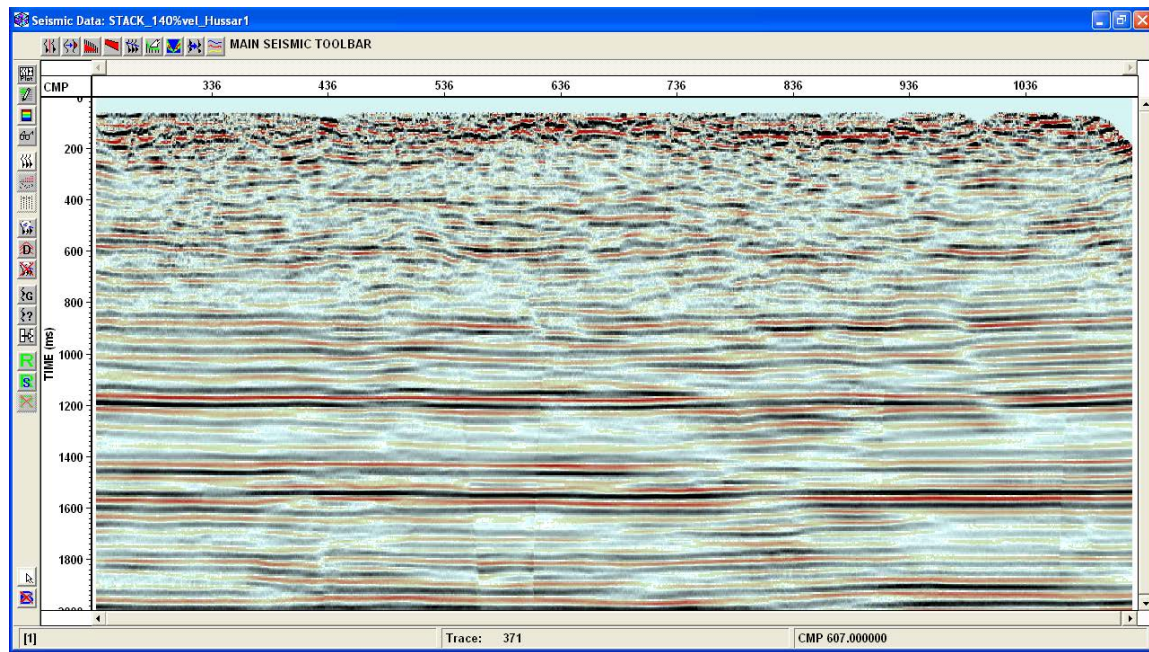


Fig. 11: Hussar data processed to 2.0 sec. using **140%** of the picked velocities.

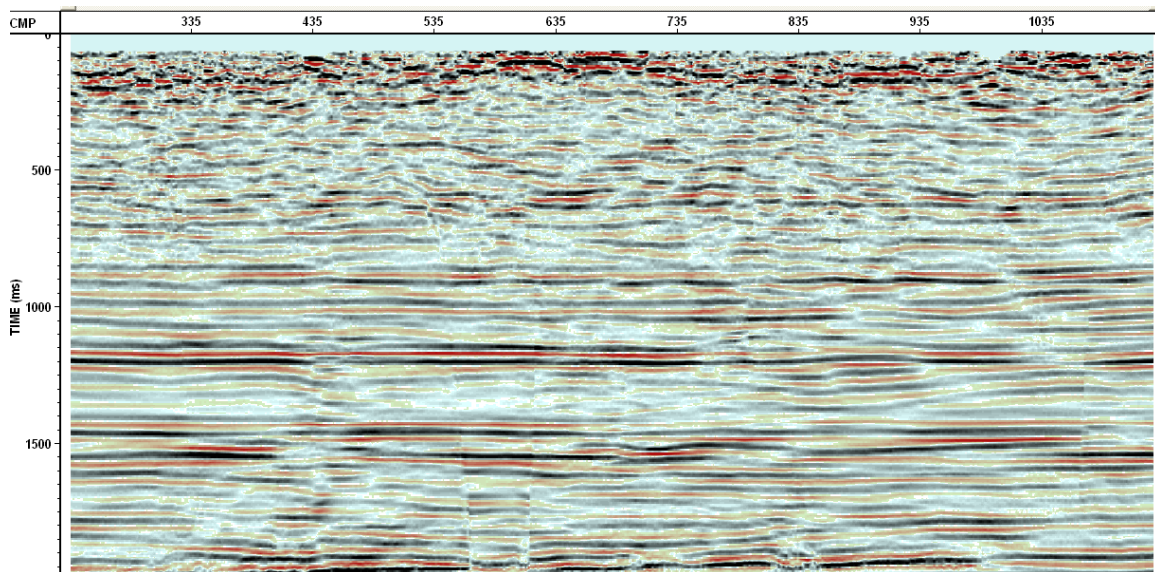


Fig. 12: Hussar data processed to 2.0 sec. using **160%** of the picked velocities.

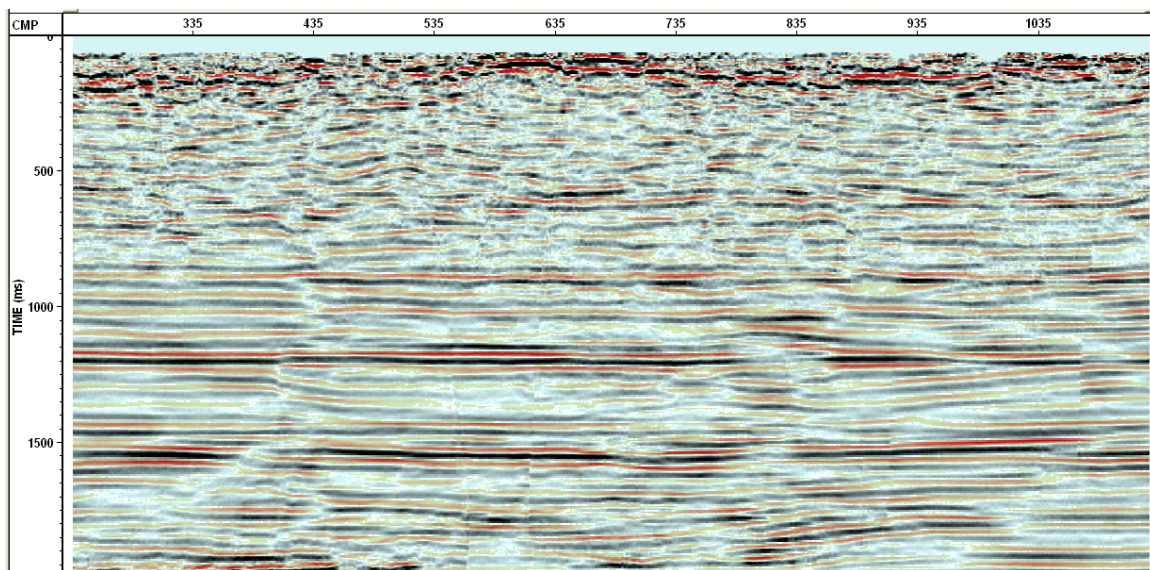


Fig. 13: Hussar data processed to 2.0 sec. using **180%** of the picked velocities.

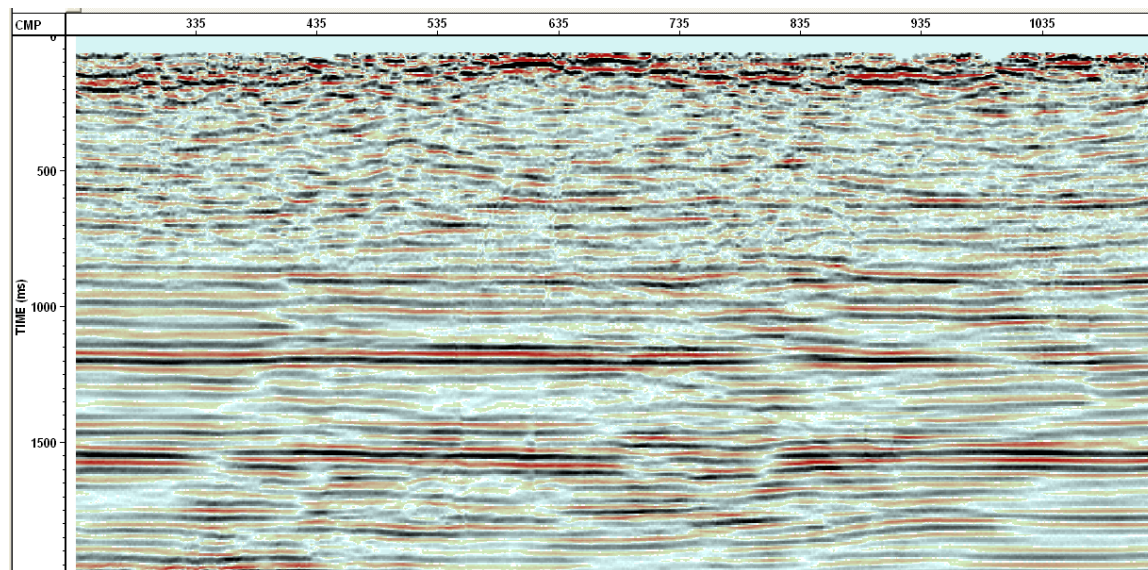


Fig. 14: Hussar data processed to 2.0 sec. using **200%** of the picked velocities.

The following are three ProMAX Kirchhoff prestack migrations processed with a horizontal datum. The velocities for each section are 100, 120, and 150 percent.

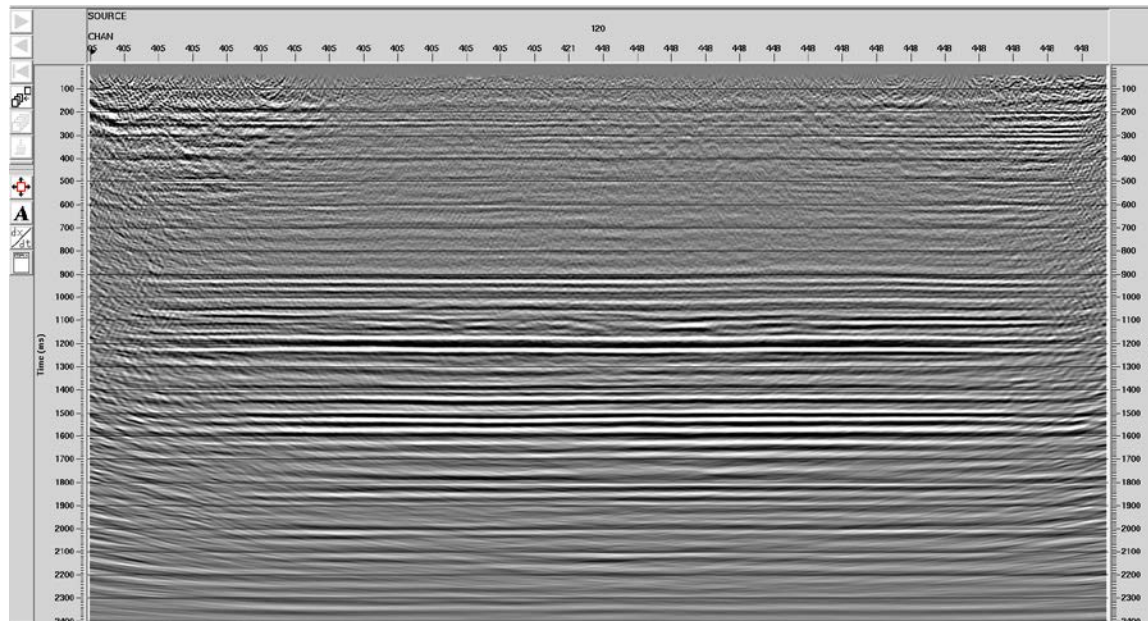


Fig. 15: Kirchhoff prestack migration using **100%** of the picked velocities.

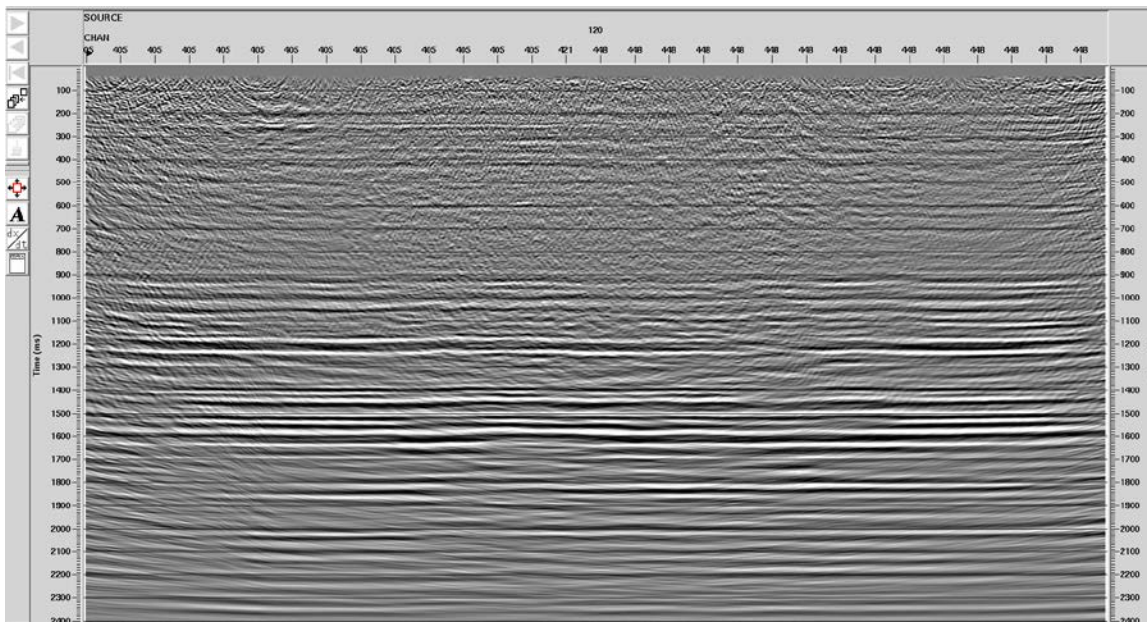


Fig. 16: Kirchhoff prestack migration using **120%** of the picked velocities.

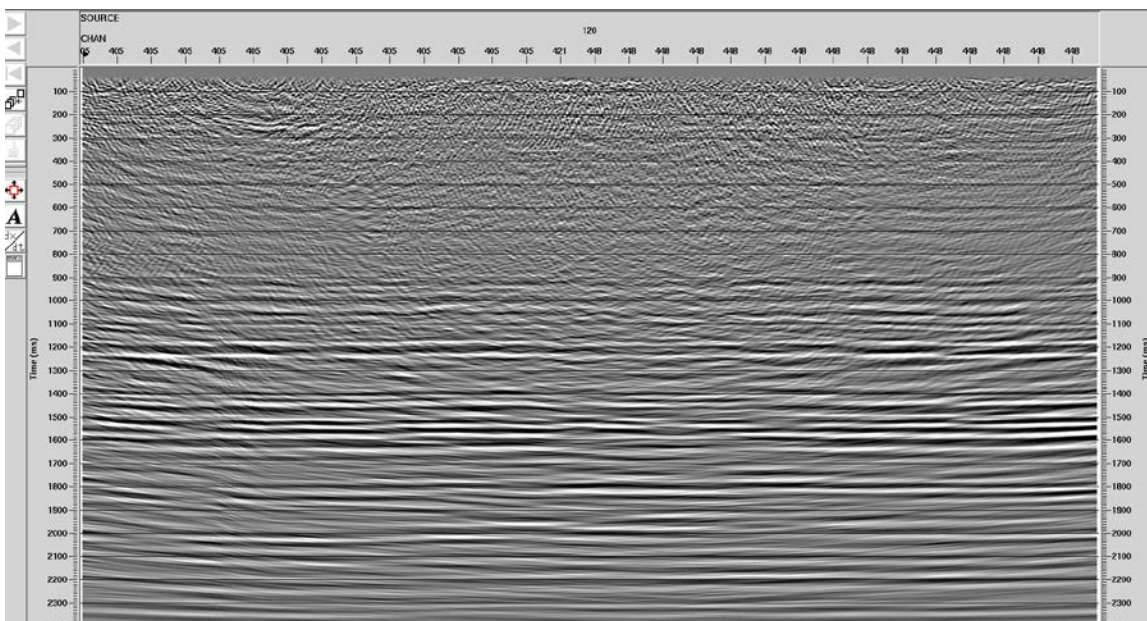


Fig. 17: Kirchhoff prestack migration using **150%** of the picked velocities.

The following are ProMAX phaseshift prestack migrations using 100, 110, 120, 130, 140, and 150 percent V_{RMS} .

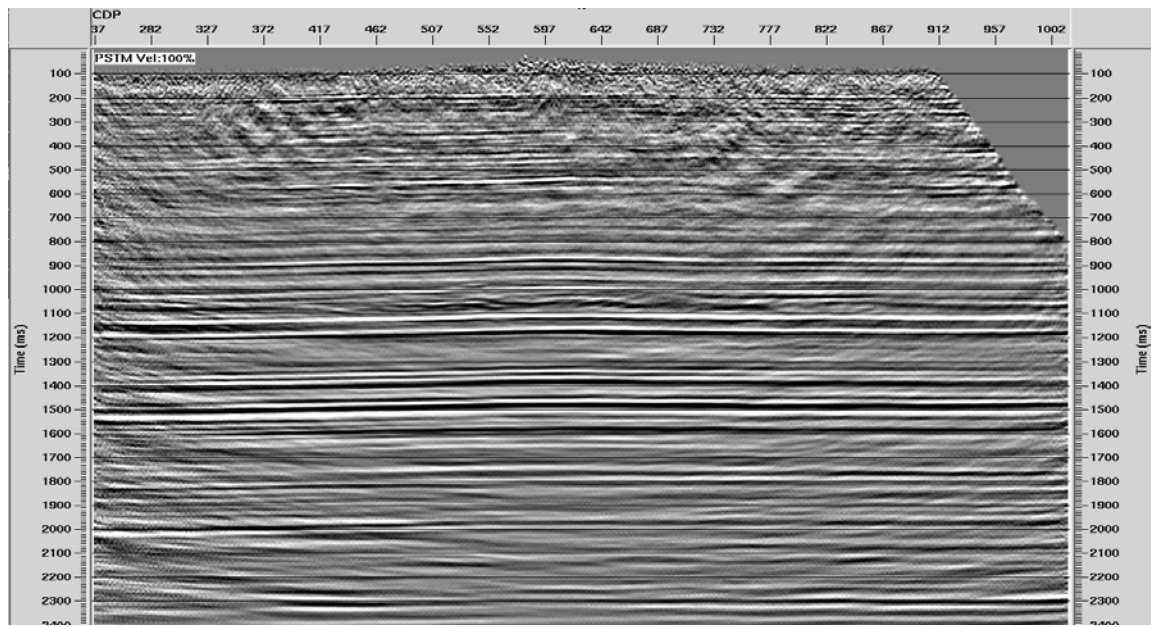


Fig. 18: Phaseshift prestack migration using **100%** of the velocities.

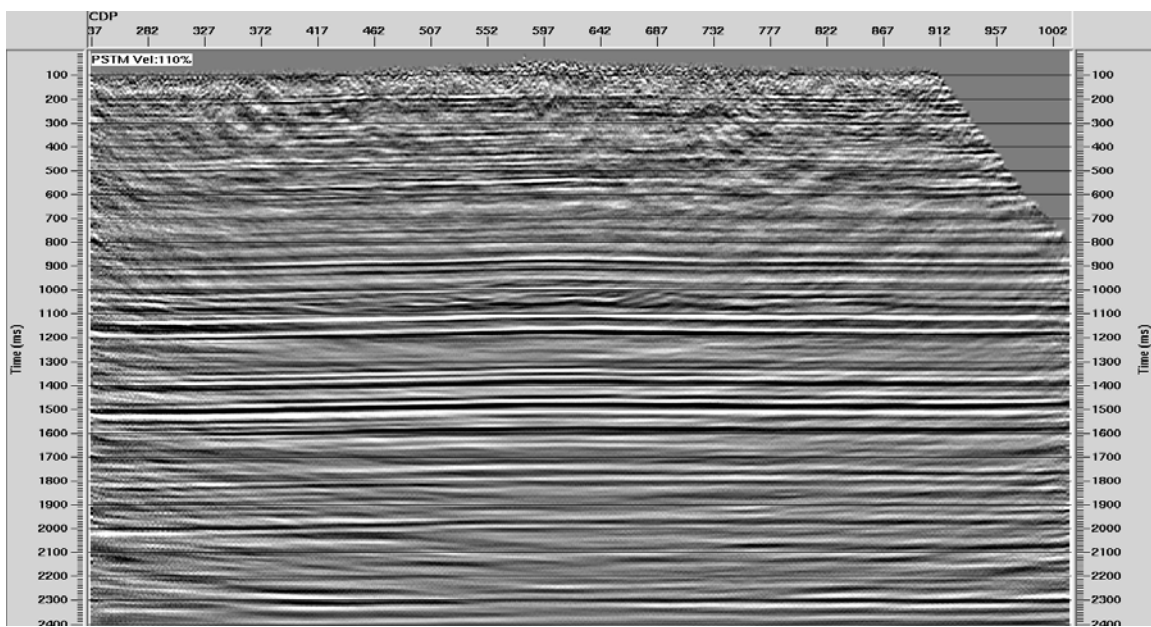


Fig. 19: Phaseshift prestack migration using **110%** of the velocities.

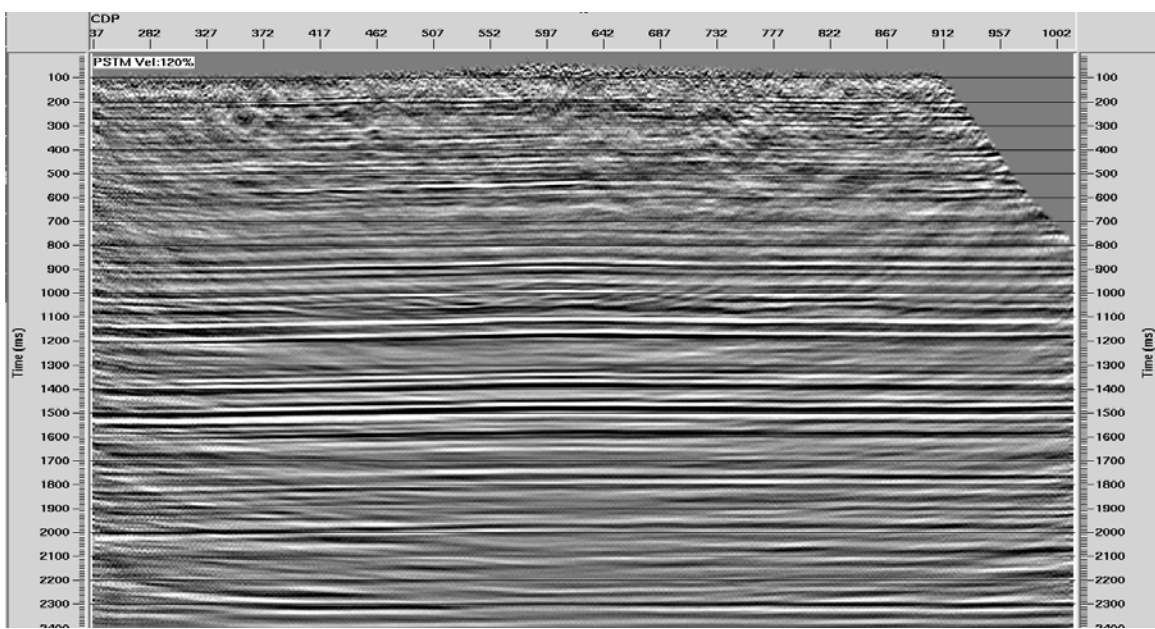


Fig. 20: Phaseshift prestack migration using **120%** of the velocities.

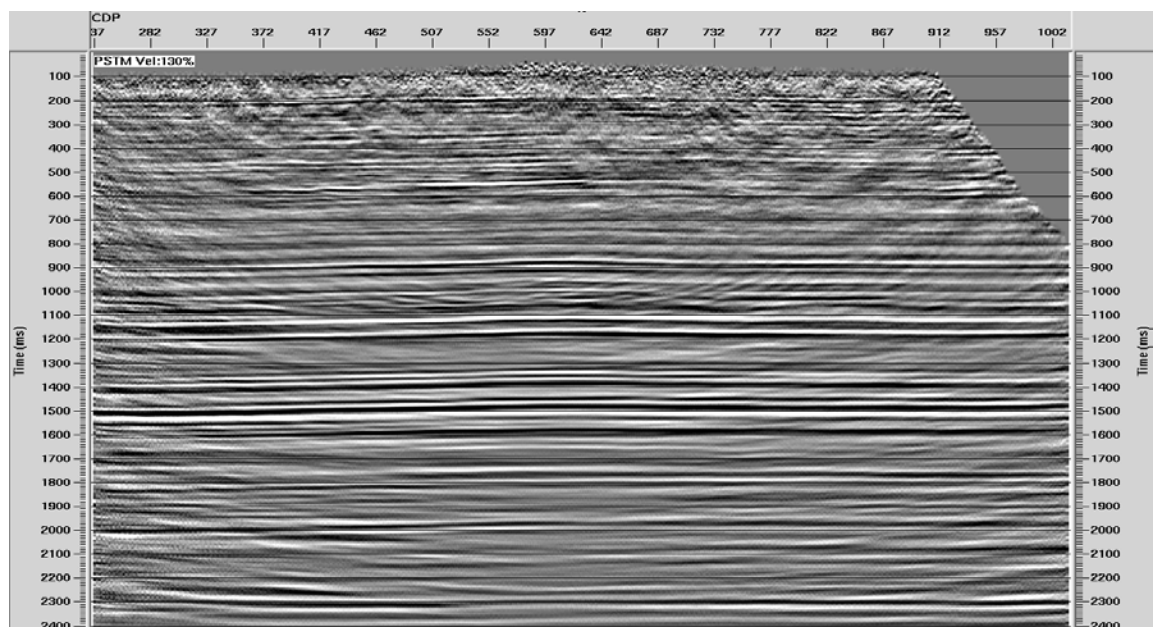


Fig. 21: Phaseshift prestack migration using **130%** of the velocities.

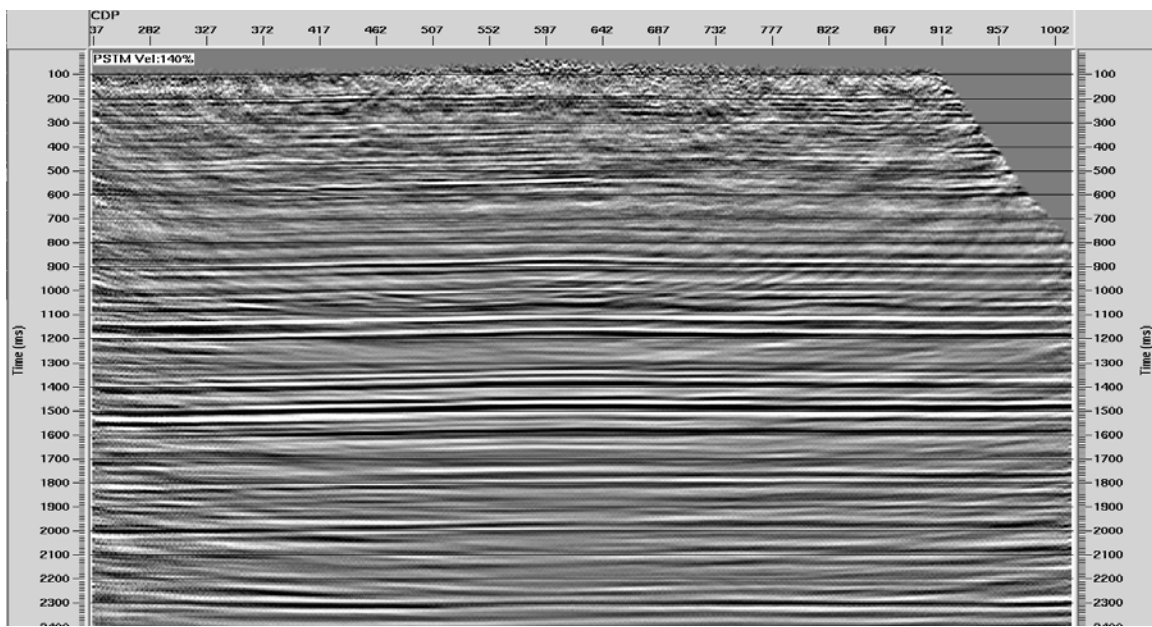


Fig. 22: Phaseshift prestack migration using **140%** of the velocities.

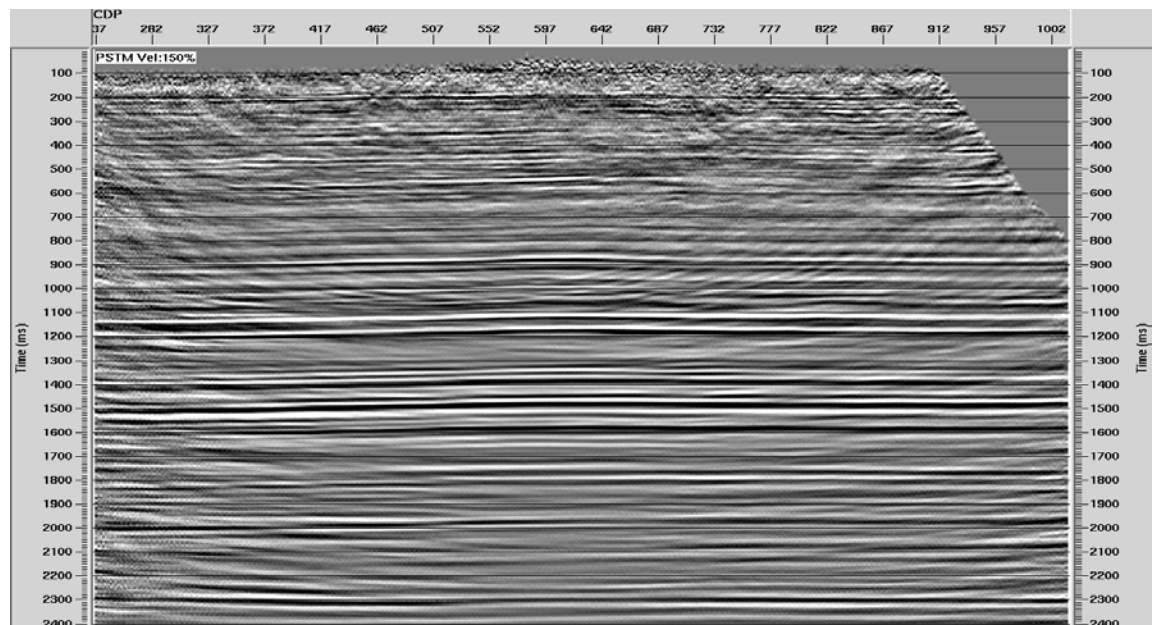


Fig. 23: Phaseshift prestack migration using **150%** of the velocities.

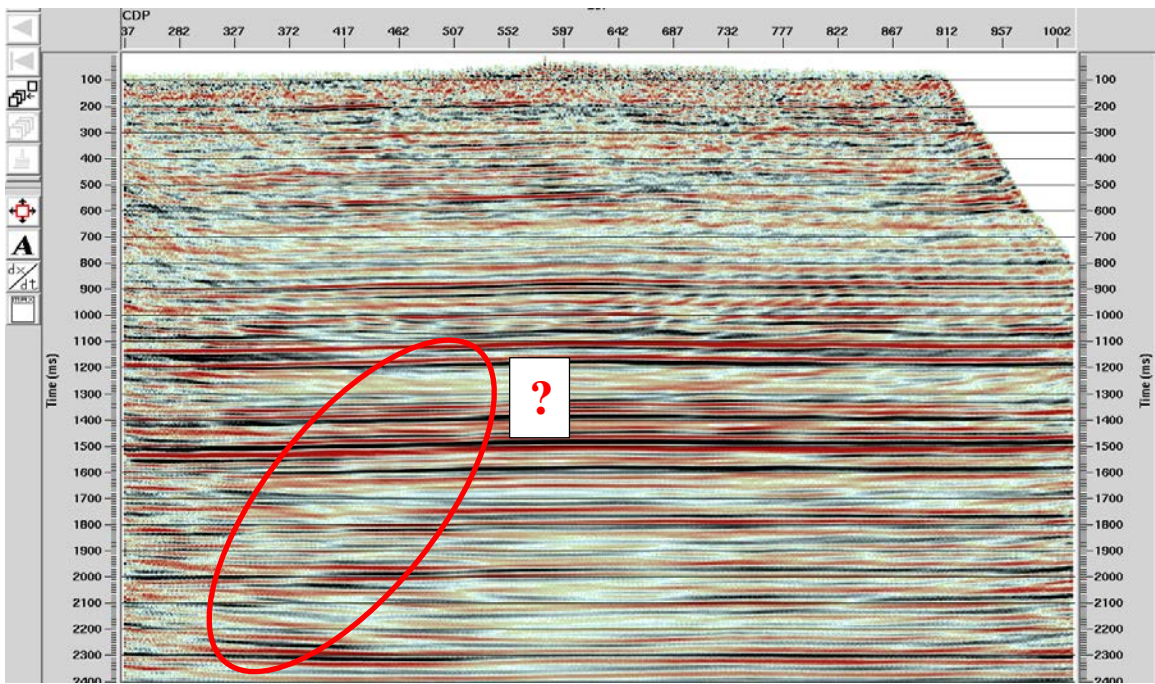


Fig. 24: Colour version of the previous prestack phase shift migration at 150% velocity.

COMMENTS AND CONCLUSIONS

The CSP gathers appear to produce prestack migrated images with high spatial resolution that appear to identify fault planes that intersect the 2D line at oblique angles. The angle of obliquity can be computed from the percent velocity that best focusses the image.

Other prestack migration algorithms were processed with the intent of verifying the images from the CSP gathers. At this time, those algorithms have failed to verify the images produced by the CSP gathers. There may be a slight hint of the faulting on the colour version of the prestack phaseshift migration using 150% in Fig. 24. When comparing Fig. 23 and Fig. 24, it appears the coloured section may provide a better visualization of the “anomalies” as indicated by the red ellipse.

The fault planes identified when using the CSP gather algorithm appear to be real and further testing is required to verify if this algorithm does produces data with high spatial resolution.

ACKNOWLEDGEMENTS

We thank the sponsors of CREWES for their support. We also gratefully acknowledge support from NSERC (Natural Science and Engineering Research Council of Canada) through the grant CRDPJ 379744-08.

REFERENCES

- Bancroft, J. C., Guirigay, T., Isaac, H., 2011, Imaging oblique reflectors on a 2D line, CREWES Research Report, Vol. 23